1 **Optically stimulated luminescence dating of Ocean Drilling Program Core 658B:**

2 **Complications arising from authigenic uranium uptake and lateral sediment movement.**

3

4 S.J. Armitage[*]

5

6 Centre for Quaternary Research, Department of Geography, Royal Holloway, University of

7 London, Egham, Surrey, TW20 0EX.

8

9 **Abstract**

10 Ocean Drilling Program Site 658 lies under the North African summer dust plume, and ought to be

11 an ideal target for optically stimulated luminescence (OSL) dating, since the main clastic input is

12 far-travelled Saharan dust. However, OSL ages for coarse silt-sized quartz (40-63 µm) are

13 systematically lower than independent age estimates when dose rates are calculated using a model

14 which assumes detrital ^{238}U, ^{232}Th and ^{40}K and excess ^{230}Th and ^{231}Pa. Ages which are in good

15 agreement with independent age control are obtained from the coarse silt samples when a correction

16 for authigenic uranium uptake is incorporated into the dose rate model. Authigenic uranium uptake

17 occurs under reducing conditions, which are common at the sediment-water interface, and some

18 degree of authigenic uranium correction may be required for most marine sediments. Using this

19 revised dose rate model, ages produced using fine silt-sized quartz (4-11 µm) are up to 100% older

20 than both independent and coarse silt ages. In addition, the fine silt ages show a consistent pattern

21 of age decrease with depth over 1.5 m of core. ^{230}Th data from Site 658 indicate that this site

22 receives 3 times more sediment laterally than vertically. It is concluded that the fine silt at Site 658

23 contains a substantial reworked component, making it unsuitable for dating. Conversely the coarse

24 silt fraction, which settles through water at ~40 times the rate of fine silt, appears to be derived from

25 dust input over the site at the time of deposition. Since prominent nepheloid (cloudy) layers occur in

[*] e-mail: simon.armitage@rhul.ac.uk

26 various deep ocean basins, and the material suspended in these layers often consists of reworked

27 fine silt-sized sediments, coarser material should be dated where possible.

28

30

1. Introduction

32 Marine sediments are one of the most widely exploited archives of palaeoenvironmental information.

33 At present, most chronologies are constructed by tuning marine proxies for global ice volume (δ^{18}O)

34 to the well understood variations in the Earth's orbit (Lisiecki and Raymo, 2005), by the identification

35 of event horizons (e.g. Sikes et al., 2000) and/or by radiocarbon dating. However, dating deep-sea

36 sediments remains problematic. Chronologies based on δ^{18}O records are dependent upon the accuracy

37 of the climate change model assumed and necessarily obscure information regarding phasing of the

38 events observed. Event horizons are only useful where their occurrence is reasonably frequent in the

39 time period of interest. In addition, both techniques require approximately continuous sedimentation,

40 and the absence of sediment reworking. Whilst a tremendously powerful geochronological tool,

41 Accelerator Mass Spectrometry (AMS) radiocarbon dating is limited to the last 50-60,000 years and

42 is subject to uncertainties due to variation in the atmospheric ^{14}C concentrations and the marine

43 carbon reservoir. The latter effect may introduce a substantial and temporally variable systematic

44 error to a chronology (Sikes et al., 2000). In addition, chronologies can only be constructed using

45 radiocarbon or the δ^{18}O record where organic carbonates are preserved, which is not the case in areas

46 with high clastic sedimentation rates (Sugisaki et al., 2010), or at sites below the carbonate

47 compensation depth. These limitations to well established dating techniques have led several authors

48 (Berger, 2006; Jakobsson et al., 2003; Stokes et al., 2003) to advocate the use of optically stimulated

49 luminescence (OSL) methods to provide age control for deep-sea sediments.

50

51   Although marine sediments were first dated using thermoluminescence techniques in 1979 (Wintle

52   and Huntley, 1979) and using OSL techniques in 2003 (Jakobsson et al., 2003; Stokes et al., 2003),

53   there are relatively few published luminescence chronologies for open ocean sediments. This absence

54   is possibly explained by the complex dose rate measurements and calculations required, due to the

55   presence of uranium-series disequilibrium in many deep sea sediments (Wintle and Huntley, 1979).

56   For many terrestrial sediments it is valid to assume that the ^{238}U, ^{235}U and ^{232}Th decay series are in

57   secular equilibrium. Consequently, dose rates due to these decay series are effectively invariant over

58   Quaternary timescales. This remains true for ^{232}Th in marine sediments since thorium is highly

59   insoluble and is incorporated into marine sediments, in equilibrium with its daughters, within the

60   detrital component. Conversely, the geochemistry of both uranium decay series makes it likely that

61   they will be in disequilibrium in late Quaternary ocean sediments. In the oxidising conditions found

62   in most seawater, uranium is highly soluble. However, long-lived isotopes in both uranium decay

63   series (^{230}Th in the ^{238}U series and ^{231}Pa in the ^{235}U series) are insoluble and are removed from the

64   water column by sorbtion to the surface of settling particles (Henderson and Anderson, 2003)

65   meaning that they are initially found in excess (relative to isotopes earlier in the relevant decay series)

66   in many marine sediments. These isotopes have half-lives which are similar to the timescales over

67   which OSL dating is applicable (75 and 32.8 ka for ^{230}Th and ^{231}Pa respectively) causing the dose

68   rate due to these isotopes and their decay products to evolve as the sediment ages. Consequently, OSL

69   dating of marine sediments is complicated by the need to demonstrate the absence of excess activity

70   in the uranium decay series (Jakobsson et al., 2003; Sugisaki et al., 2010; Sugisaki et al., 2012) or to

71   quantify excess activity and incorporate the resulting time-dependant dose rate changes into age

72   calculations (Stokes et al., 2003; Wintle and Huntley, 1979). This study compares AMS ^{14}C and

73   quartz OSL chronologies produced for a core from Ocean Drilling Program (ODP) Site 658.

74

75   **2 Materials and methods**

76   Core 658B was the second of three cores recovered from a water depth of 2,263 m off Cap Blanc,

77   Mauritania (20°45'N, 18°35'W) during ODP Leg 108 (Ruddiman et al., 1988). Trade winds cause

78   strong upwelling over the site, leading to high surface productivity and high biogenic particle fluxes

79   to the seafloor. Biogenic carbonate comprises 40-60% by mass of the sediment, with the remainder

80   being terrigenous dust (deMenocal et al., 2000). The high terrigenous dust flux is due to the site's

81   location beneath the axis of the summer African dust plume (Figure 1). Core 658B is an ideal target

82   for testing OSL dating in the marine realm since: (1) It has a high accumulation rate (c.18 cm/ka,

83   deMenocal et al., 2000); (2) Terrigenous dust input should provide a substantial well-bleached

84   quartz component; (3) Neighbouring core 658C has a well dated dust flux record covering the last

85   22 ka (deMenocal et al., 2000) and (4) the excess ^{230}Th (^{230}Th$_{xs}$) record for core Core 658C (Adkins

86   et al., 2006) may be used to calculate excess activity in Core 658B.

87

88   Independent chronological data for Core 658B were obtained from two sources. Firstly, 18 samples

89   from core depths ranging from ~2.3-10.9 m (effectively the upper ~8.5 m of core since the

90   uppermost 2.3 m appears to replicate underlying material) were dated by AMS ^{14}C on 150-250 μm

91   *Globigerinoides bulloides* tests. Fifteen of these AMS ^{14}C measurements yielded finite ages (Table

92   S1). Secondly, dated stratigraphic markers in Core 658C (deMenocal et al., 2000) and the LR04

93   benthic δ^{18}O stack (Lisiecki and Raymo, 2005) were identified in Core 658B (Table S2). Both

94   approaches yield a similar age-depth relationship, though the Core 658B AMS ^{14}C ages show age

95   inversions especially below 7 m, towards the upper limit of the technique (Figure 2). There is no

96   apparent lithological change at 7 m, and it is possible that the age inversions are due to reworking of

97   foraminiferal tests or variable reservoir effects.

98

99   **2.1 Equivalent dose determination**

100   Samples were obtained from a 66 mm diameter split core at the ODP East Coast Repository,

101   Lamont-Doherty Earth Observatory, USA. Since collection in 1986, the core had been refrigerated

102 and kept moist via damp sponges inserted at the ends of each core section, but no attempt had been

103 made to shield the core from light. Paired samples were taken every ~25 cm through the uppermost

104 11 m of the core by inserting short sections of 20 mm diameter opaque tubing. Under subdued

105 orange lighting the sediment was extruded and the outer ~8 mm was discarded to avoid core barrel

106 smearing. The light exposed upper ~8 mm was removed and used for carbonate content and dose

107 rate analysis. The middle ~8 mm of the sample was dispersed in deionised water and sieved at 150

108 μm, with the >150 fraction consisting of foraminiferal tests, and the <150 μm fraction being used

109 for dating. The dating fraction was sequentially treated with HCl, H_2O_2 and H_2SiF_6 to remove

110 carbonate, organic matter and feldspars respectively. The resulting mixture was separated into fine

111 silt (4-11 μm) and coarse silt (40-63 μm where present) fractions via Stokes settling and wet sieving

112 respectively.

113

114 All OSL measurements presented in this study were carried out using a Risø TL/OSL-DA-15

115 automated dating system (Bøtter-Jensen et al., 2000). Optical stimulation of single aliquots was

116 carried out using a blue (470 ± 30 nm) light emitting diode (LED) array with a nominal power density

117 of 18 mW/cm^2. Infra-red (IR) stimulation was carried out using an IR (870 nm) laser diode array.

118 OSL was measured using an Electron Tubes Ltd 9235QB photomultiplier tube with 7.5 mm of Hoya

119 U-340 filter interposed between the sample and photomultiplier. Irradiation was carried out using a

120 40 mCi ^{90}Sr/^{90}Y beta source, calibrated relative to the National Physical Laboratory, Teddington

121 Hotspot 800 ^{60}Co γ-source (Armitage and Bailey, 2005). Single-aliquot equivalent doses (D_e) were

122 determined using the single-aliquot regenerative-dose (SAR) method (Galbraith et al., 1999; Murray

123 and Wintle, 2000). OSL signals were measured at 125 °C and growth curves were fitted using a

124 saturating exponential function. No dependence of D_e upon preheating regime was found (Figure S1)

125 and a preheating regime of 260 °C, 10 s for PH1 (the pre-heat prior to measurement of L_n or L_x) and

126 220 °C, 10 s for PH2 (the pre-heat prior to measurement of T_n or T_x) was adopted for subsequent

127 measurements. Dose recovery experiments (Roberts et al., 1999; Wallinga et al., 2000) were

128   performed on the coarse silt fractions of samples 11B, 19A and 27A (D_e = 23, 44 and 77 Gy

129   respectively) using this preheating regime, yielding dose recovery ratios of 0.99 ± 0.01, 0.98 ± 0.01

130   and 0.98 ± 0.01 respectively. When calculating D_e, aliquots were rejected where the recycling ratio

131   (Murray and Wintle, 2000) or IR depletion ratio (Duller, 2003) differed from unity by more than two

132   standard deviations, or where the sensitivity corrected luminescence intensity in response to a 0 Gy

133   regeneration dose exceeded 5% of the sensitivity corrected natural luminescence intensity (Table S3).

134

135   **2.2 Dose rate detremination**

136   The environmental dose rate for samples from core 658B consists of alpha, beta and gamma

137   components, since the overlying water completely shields the ocean floor sediments from cosmic

138   rays. ^{238}U and ^{232}Th and bulk K concentrations were measured using ICP-MS (Table S4). Burial

139   ^{230}Th$_{xs}$ for all samples was assumed to be the mean value (36.6±9.3 Bq/kg) measured by Adkins et

140   al. (2006) for Core 658C over the time period 2-18.5 ka. Adkins et al. (2006) determined ^{230}Th$_{xs}$

141   using a VG Plasma Quad 2 ICP-MS, reporting <1% counting statistics errors and 0.17 Bq/kg

142   procedural blanks. Initial ^{231}Pa$_{xs}$ (3.38±0.87 Bq/kg) was calculated using the 0.093 production

143   activity ratio of ^{231}Pa/^{230}Th (Henderson and Anderson, 2003). Time independent dose rates were

144   calculated from ^{238}U and ^{232}Th and K concentrations, assuming equilibrium in both decay series,

145   using the standard conversion factors (Adamiec and Aitken, 1998). The additional time dependant

146   dose contribution due to ^{230}Th$_{xs}$ and ^{231}Pa$_{xs}$, and the final age calculation, were performed using the

147   method outlined by Stokes et al. (2003). Both coarse and fine silt dose rates were corrected for

148   alpha efficiency (0.04±0.02), alpha and beta attenuation and water content (Aitken, 1985). Water

149   contents were taken from the relevant ODP initial report (Ruddiman et al., 1988). The above dose

150   rate calculation is referred to as the "Marine$_{xs}$" dose rate model hereafter. Dose rates and ages

151   calculated using the Marine$_{xs}$ model are presented in Table S5.

152

153   **3 Results and discussion**

154   Coarse silt OSL ages calculated using the Marine$_{xs}$ model are shown alongside the independent

155   chronological data in Figure 2. It is clear that the coarse silt OSL ages underestimate the

156   independent ages by a considerable amount.

157

158   Whilst uranium forms soluble species in oxidising conditions, under suboxic or anoxic conditions it

159   is reduced to its insoluble tetravalent state (Henderson and Anderson, 2003). This situation

160   frequently occurs at or near the sediment-water interface, resulting in the incorporation of

161   authigenic uranium in marine sediments. Especially high authigenic uranium concentrations occur

162   where high surface productivity leads to a high organic matter flux to the sea bed, since this

163   material consumes oxygen during its decay (Henderson and Anderson, 2003). Consequently it

164   might be expected that sediments from ODP site 658 will have a high authigenic uranium content.

165   Authigenic uranium isotopes ($^{238}U_{auth}$ and $^{234}U_{auth}$) are incorporated into marine sediment at the

166   seawater activity ratio of $^{234}U/^{238}U = 1.146$ (Robinson et al., 2004), and without any supported

167   decay products. For dating purposes, $^{238}U_{auth}$ instantly attains equilibrium with the next two decay

168   products (^{234}Th and ^{234}Pa) since neither is long-lived. Conversely, ^{234}U has a half-life of 245 ka and

169   hence will not approach equilibrium with its parent (^{234}Pa) over the applicable age range of quartz

170   OSL dating. However, since authigenic uranium is incorporated into the sediment at an activity

171   ratio of $^{234}U/^{238}U$ of 1.146, $^{234}U_{auth}$ may be treated as being in equilibrium with $^{238}U_{auth}$ for the

172   purposes of estimating dose rates. The slight excess activity of $^{234}U_{auth}$ over $^{238}U_{auth}$ has a negligible

173   impact upon dose rates since the decay of ^{234}U contributes a small proportion of the dose rate due to

174   the ^{238}U decay series (11% of alpha, 0.5% of beta and 0.1% of gamma). Since both ^{234}U and its

175   decay product ^{230}Th are long-lived (half-lives of 245 and 75 ka respectively), the ingrowth of

176    $^{234}U_{auth}$ decay products is negligible over the 0-50 ka timeframe covered by this study.

177   Consequently, in this study the dose rate due to authigenic uranium may be approximated by

178   assuming secular equilibrium from $^{238}U_{auth}$-$^{234}U_{auth}$, and no dose from the decay products of $^{234}U_{auth}$.

179   Since most of the alpha, beta and gamma energy in the ^{238}U decay series is emitted at or below ^{234}U

180   (Stokes et al., 2003), the dose rate must be corrected to account for authigenic uranium uptake

181   where it occurs.

182

183   The authigenic uranium content of a marine sediment may be calculated from the measured ^{238}U

184   and ^{232}Th activities (or the activities calculated from the measured concentrations), since the ^{232}Th

185   is entirely detrital, and the ^{238}U/^{232}Th activity ratio of crustal rocks and pelagic marine sediments is

186   0.8±0.2 (Anderson et al., 1989). Equation 1 was used to calculate authigenic uranium contents of

187   Core 658B samples

188

189   $U_{auth} = {}^{238}U_m - 0.8 * {}^{232}Th_m$ (Eq. 1)

190

191   where $^{238}U_m$ and $^{232}Th_m$ are the measured activities of ^{238}U and ^{232}Th respectively (Yu et al., 1999).

192   This calculation was performed for all samples in this study (n=29), adding a 20% uncertainty to the

193   U_{auth} activity, and the mean $^{238}U_{auth}/^{238}U_m$ ratio was 0.77±0.18. In the Marine$_{xs}$ dose rate model, the

194   entire detrital ^{238}U decay series is assumed to be in equilibrium, which will result in an overestimate

195   of the true dose rate due to uranium where authigenic uranium uptake has occurred. Ages were

196   recalculated using the revised "Marine$_{xs+auth}$" dose rate model, in which the dose rate due to $^{238}U_{auth}$

197   is calculated assuming equilibrium to ^{234}U, with no dose from the decay products of $^{234}U_{auth}$, and the

198   detrital ^{238}U ($^{238}U_m - {}^{238}U_{auth}$) decay series is assumed to be in equilibrium throughout. In the

199   Marine$_{xs+auth}$ dose rate model, all other components are calculated as in the Marine$_{xs}$ dose rate

200   model. Coarse silt OSL ages calculated using the Marine$_{xs+auth}$ dose rate model (Table S6) are in

201   good agreement with the independent chronological data (Figure 3a), indicating that the age

202   underestimation observed when using the Marine$_{xs}$ dose rate model is caused by the failure of this

203   model to account for authigenic uranium uptake. The mean ratio of Marine$_{xs}$/ Marine$_{xs+auth}$ dose rate

204   ages is 0.73±0.05.

205

206   Ages were calculated, using the Marine$_{xs+auth}$ dose rate model, for the 16 samples for which

207   equivalent doses had been measured on fine quartz silt (Table S7, Figure 3b). The fine silt ages do

208   not increase monotonically with depth, nor do they agree with the independent chronological data

209   or the paired coarse silt ages where available (~4-6.5 m). All fine silt OSL ages are older than

210   corresponding coarse silt OSL ages and independent age control. Together these discrepancies are

211   taken to indicate that the dose rate model is correct, but that the fine silt equivalent doses do not

212   represent the dose experienced since the deposition of these particles at ODP Site 658. It has been

213   suggested that in many marine contexts coarse silt might be preferential to fine silt for dating since

214   90% of grains within the nepheloid (cloudy) layer in non-polar deep oceans, which results from

215   sediment reworking, consist of grains with a diameter of 0.5-8.5 µm (Berger, 2006). Also, the

216   ^{230}Th$_{xs}$ record from ODP core 658C indicates that over the last 20 ka, this site has received 3 times

217   more sediment laterally than vertically, though this ratio is quite variable (Adkins et al., 2006).

218   Since 50 µm grains settle through water at ~40 times the rate of 8 µm grains, the coarse silt fraction

219   is more likely to be incorporated via sea surface aeolian input immediately prior to deposition than

220   is the fine silt fraction. Consequently, the discrepancy between coarse silt and fine silt OSL ages at

221   site 658B is attributed to ocean floor reworking, without exposure to sunlight, of the latter.

222

223   **4 Conclusions**

224   Disequilibrium in the ^{238}U and ^{235}U decay series due to precipitation of insoluble isotopes from the

225   water column is a well-known phenomenon in marine sediments (Wintle and Huntley, 1979). With

226   appropriate ^{230}Th$_{xs}$ measurements, the effect of this disequilibrium on dose rates can be accounted

227   for (Stokes et al., 2003). At ODP Site 658, authigenic uranium uptake represents an important

228   additional source of disequilibrium. A simple dose rate correction is proposed, which appears

229   suitable for sediments which are much younger than the half-life of ^{234}U. However, more complex

230   dose rate corrections will be required in older samples where significant ingrowth of ^{234}U$_{auth}$ decay

231   products has occurred. It is probable that authigenic uranium uptake in marine sediments could

232 disguise quite large ^{230}Th$_{xs}$ activities where secular equilibrium is diagnosed on the basis of

233 ^{226}Ra/^{238}U activity ratios determined using high-resolution gamma spectrometry (e.g. Jakobsson et

234 al., 2003). Consequently, it is prudent to calculate authigenic uranium uptake for all samples when

235 dating open ocean sediments.

236

237 Coarse silt (40-63 µm) OSL ages from site 658B are internally consistent and in good agreement

238 with independent age control. Conversely, fine silt (4-11 µm) yielded older ages for all samples,

239 and dates did not increase monotonically with depth. It appears likely that seafloor reworking of

240 fine silt caused these ages to be unrepresentative of the timing of sediment formation at the sampled

241 position. This result potentially limits the applicability of OSL dating to marine sediments, since the

242 coarse silt component at site 658B results from its location under the North African summer dust

243 plume. However, since the deep ocean nepheloid layer contains little material >10 µm, it is possible

244 that accurate ages for sediment formation could be obtained from silts only slightly coarser than the
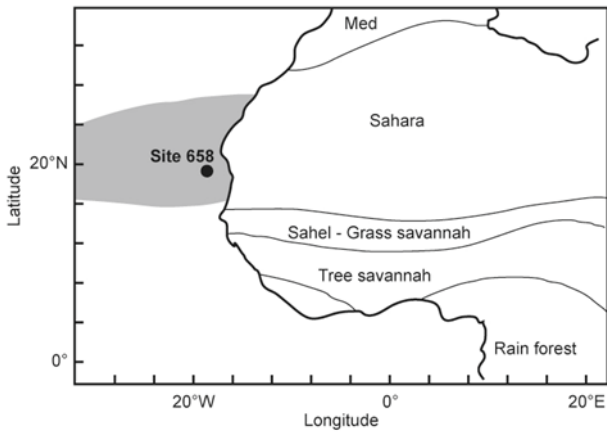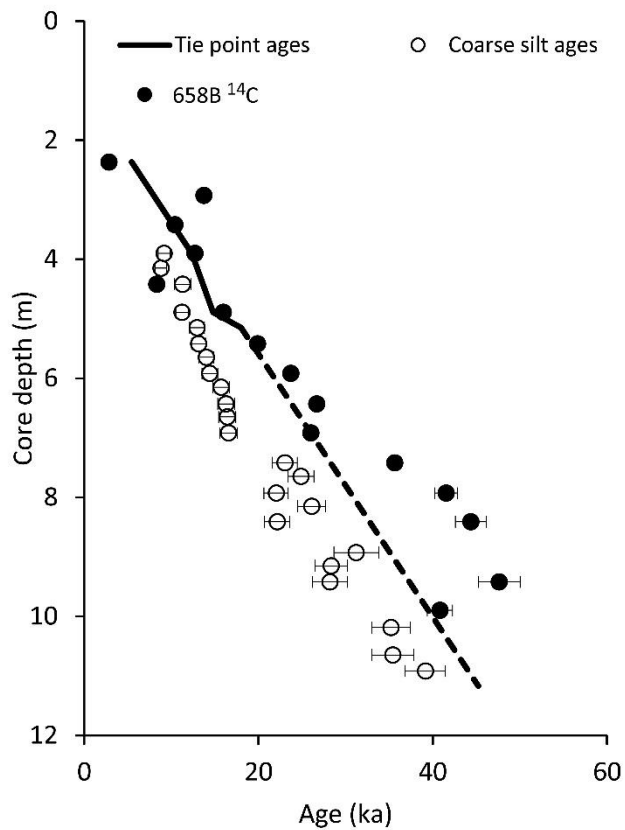
245 4-11 µm fraction measured here.

246

254 **Figures**

255

256

257 Figure 1: Location of ODP Site 658 under the summer African dust plume (grey). Redrawn from

258 deMenocal et al. (2000).

259

Figure 2: Chronological models for Core 658B. Filled circles represent independent age estimates determined using AMS ^{14}C on foraminifera from Core 658B and the solid line represents an age-depth relationship determined by matching stratigraphic events to external dated stratigraphies, assuming constant sedimentation between these tie points. The dashed line represents the age-depth relationship beyond 18 ka, assuming that the 22 cm/ka sedimentation rate observed between 2.37 and 5.15 m core depth continues. Open circles represent coarse silt OSL ages calculated using the Marine$_{xs}$ dose rate model.
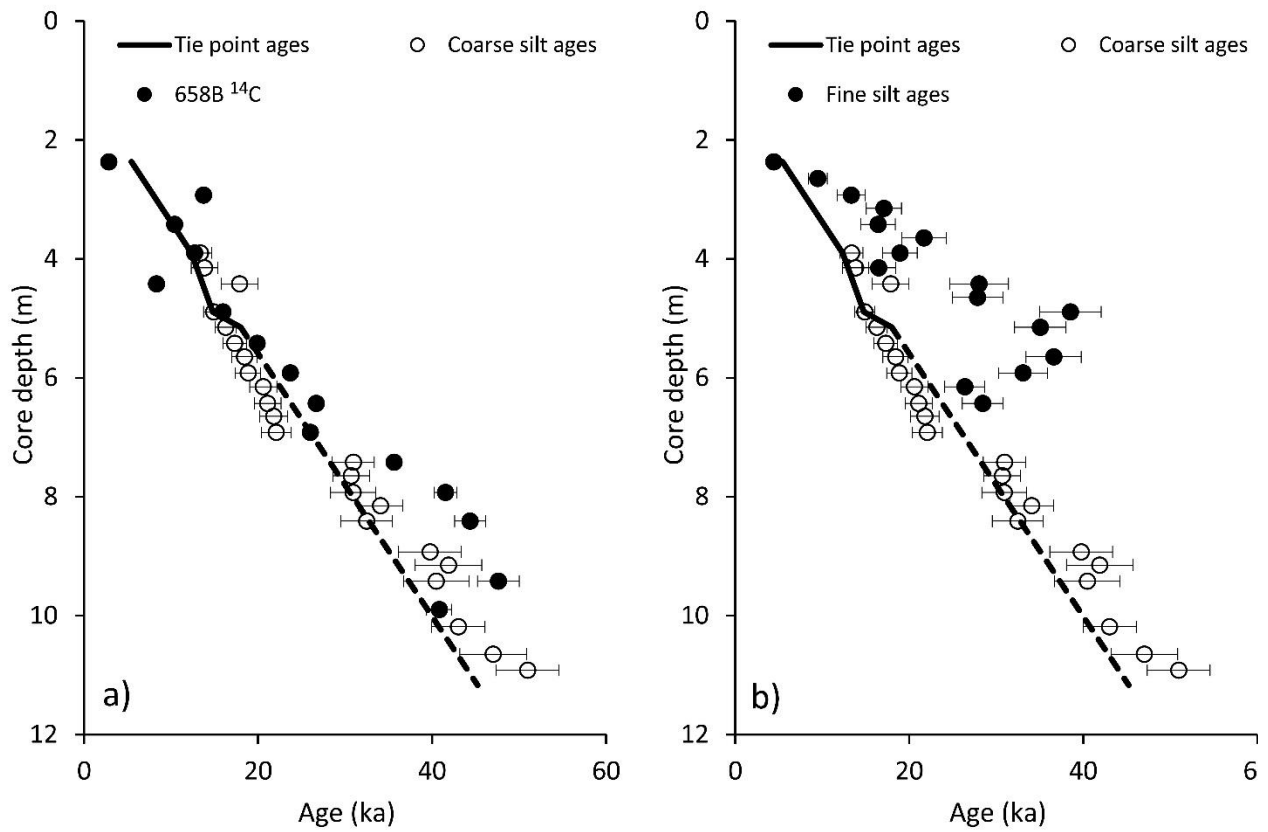
Figure 3: Independent age estimates and OSL ages for Core 658B. a) Independent age estimates and coarse silt OSL ages calculated using the Marine$_{xs+auth}$ dose rate model. b) Coarse silt and fine silt OSL ages calculated using the Marine$_{xs+auth}$ dose rate model, plotted alongside the independent age-depth model. Core 658B AMS ^{14}C ages have been removed from panel b for clarity.

274 **References**
275
276 Adamiec, G., Aitken, M., 1998. Dose-rate conversion factors: update. Ancient TL 16, 37-50.
277 Adkins, J., deMenocal, P., Eshel, G., 2006. The "African humid period" and the record of marine
278 upwelling from excess 230Th in Ocean Drilling Program Hole 658C. Paleoceanography 21.
279
280 Aitken, M.J., 1985. Thermoluminescence dating. Academic press.
281
282 Anderson, R.F., Lehuray, A.P., Fleisher, M.Q., Murray, J.W., 1989. Uranium deposition in saanich
283 inlet sediments, vancouver island. Geochimica et Cosmochimica Acta 53, 2205-2213.
284
285 Armitage, S.J., Bailey, R.M., 2005. The measured dependence of laboratory beta dose rates on
286 sample grain size. Radiat Meas 39, 123-127.
287
288 Berger, G.W., 2006. Trans-arctic-ocean tests of fine-silt luminescence sediment dating provide a
289 basis for an additional geochronometer for this region. Quaternary Science Reviews 25, 2529-2551.
290
291 Bøtter-Jensen, L., Bulur, E., Duller, G.A.T., Murray, A.S., 2000. Advances in luminescence
292 instrument systems. Radiat Meas 32, 523-528.
293
294 deMenocal, P., Ortiz, J., Guilderson, T., Adkins, J., Sarnthein, M., Baker, L., Yarusinsky, M., 2000.
295 Abrupt onset and termination of the African Humid Period: Rapid climate responses to gradual
296 insolation forcing. Quaternary Science Reviews 19, 347-361.
297
298 Duller, G.A.T., 2003. Distinguishing quartz and feldspar in single grain luminescence
299 measurements. Radiat Meas 37, 161-165.
300
301 Galbraith, R.F., Roberts, R.G., Laslett, G.M., Yoshida, H., Olley, J.M., 1999. Optical dating of
302 single and multiple grains of quartz from Jinmium rock shelter, northern Australia: Part I,
303 experimental design and statistical models. Archaeometry 41, 339-364.
304
305 Henderson, G.M., Anderson, R.F., 2003. The U-series toolbox for palaeoceanography, in: Bourdon,
306 B., Henderson, G.M., Lundstrom, C.C., Turner, S.P. (Eds.), Uranium-series geochemistry.
307 Geochemical Society and Mineralogical Society of America, Washington, p. 656.
308
309 Jakobsson, M., Backman, J., Murray, A., Løvlie, R., 2003. Optically stimulated luminescence
310 dating supports central arctic ocean cm-scale sedimentation rates. Geochemistry, Geophysics,
311 Geosystems 4.
312
313 Lisiecki, L.E., Raymo, M.E., 2005. A Pliocene-Pleistocene stack of 57 globally distributed benthic
314 δ 18O records. Paleoceanography 20, 1-17.
315
316 Murray, A.S., Wintle, A.G., 2000. Luminescence dating of quartz using an improved single-aliquot
317 regenerative-dose protocol. Radiat Meas 32, 57-73.
318
319 Roberts, R.G., Galbraith, R.F., Olley, J.M., Yoshida, H., Laslett, G.M., 1999. Optical dating of
320 single and multiple grains of quartz from Jinmium rock shelter, northern Australia: Part II, results
321 and implications. Archaeometry 41, 365-395.
322
323 Robinson, L.F., Belshaw, N.S., Henderson, G.M., 2004. U and Th concentrations and isotope ratios
324 in modern carbonates and waters from the Bahamas. Geochimica et Cosmochimica Acta 68, 1777-
325 1789.

326   Ruddiman, W., Sarnthein, M., Baldauf, J., al., e., 1988. Proceedings of the Ocean Drilling Program
327   Part A - Initial Reports.
328
329   Sikes, E.L., Samson, C.R., Guilderson, T.P., Howard, W.R., 2000. Old radiocarbon ages in the
330   southwest Pacific Ocean during the last glacial period and deglaciation. Nature 405, 555-559.
331
332   Stokes, S., Ingram, S., Aitken, M.J., Sirocko, F., Anderson, R., Leuschner, D., 2003. Alternative
333   chronologies for Late Quaternary (Last Interglacial-Holocene) deep sea sediments via optical dating
334   of silt-sized quartz. Quaternary Science Reviews 22, 925-941.
335
336   Sugisaki, S., Buylaert, J.P., Murray, A., Tsukamoto, S., Nogi, Y., Miura, H., Sakai, S., Iijima, K.,
337   Sakamoto, T., 2010. High resolution OSL dating back to MIS 5e in the central Sea of Okhotsk.
338   Quat Geochronol 5, 293-298.
339
340   Sugisaki, S., Buylaert, J.P., Murray, A.S., Harada, N., Kimoto, K., Okazaki, Y., Sakamoto, T.,
341   Iijima, K., Tsukamoto, S., Miura, H., Nogi, Y., 2012. High resolution optically stimulated
342   luminescence dating of a sediment core from the southwestern Sea of Okhotsk. Geochemistry,
343   Geophysics, Geosystems 13.
344
345   Wallinga, J., Murray, A., Duller, G., 2000. Underestimation of equivalent dose in single-aliquot
346   optical dating of feldspars caused by preheating. Radiat Meas 32, 691-695.
347   Wintle, A.G., Huntley, D.J., 1979. Thermoluminescence dating of a deep-sea sediment core. Nature
348   279, 710-712.
349
350   Yu, E.F., Liang, C.H., Chen, M.T., 1999. Authigenic uranium in marine sediments of the Benguela
351   current upwelling region during the last glacial period. Terrestrial, Atmospheric and Oceanic
352   Sciences 10, 201-214.
353